DESCRIPTION AND ANALYSIS OF A LARGE DIAMETER CARBON STEEL ELBOW EXPERIMENT WITH A LONGITUDINAL SURFACE CRACK

P. Le Delliou * and C. Couterot *

In order to conduct successfully bending tests on aged cast duplex stainless steel elbows, a preliminary test on a 609 mm diameter carbon steel elbow has been performed . The elbow contained a longitudinal semi-elliptical notch on one flank. This paper describes the test facility, the experimental results and the ductile fracture analyses performed. Despite the large applied displacement, no initiation of the crack occured. The simplified J-estimation scheme used to calculate J concludes presently to the initiation, but this method contains a large conservatism. So, a non linear finite element calculation of J will be made for definite conclusion.

INTRODUCTION

Electricité De France, in cooperation with the French Atomic Energy Commission (CEA) and Framatome, is currently conducting a research program on the fracture behaviour of aged cast duplex stainless steels. The main task of this program consists in testing two aged cast elbows under closure bending [1]. The elbows will contain a semi-elliptical surface crack.

In order to conduct these tests successfully, a preliminary test on a 609 mm diameter carbon steel elbow has been performed. This paper presents the test facility, the experimental results and the ductile fracture analyses performed.

* Electricité De France (EDF), Direction des Etudes et Recherches, Dpt MTC, Les Renardières, 77250 MORET s/LOING, FRANCE

TESTS

Elbow test

The 90 degrees elbow contains a longitudinal semi-elliptical crack on the outer surface of one flank and is loaded under in-plane closure bending. Due to the ovalization effect, the crack is submitted to tensile stresses, so it may initiate and subsequently grow by ductile tearing. The elbow is made of A48 carbon steel. Its dimensions are :

external diameter : 609 mm
thickness : 50 mm
bend radius : 914 mm

Test facility. One end of the elbow is fixed to a rigid welded frame, the other one being fitted with a 6.5 m long straight pipe used as a moment arm (figure 1). The moment loading is generated by pulling on the pipe with a long stroke ram. Two A42 carbon steel connecting pipes are inserted, respectively between the elbow and the 6 m long pipe and between the elbow and the flange. The flange, the welded frame and the long pipe are made of a high elastic limit carbon steel.

Crack geometry. Figure 2 shows the crack geometry. The semi-elliptical crack has a length 2c = 250 mm and a maximum depth a = 12.5mm. The ratio c/a = 10 was chosen in order to ensure in-depth propagation. The flaw was made by electric decharge machining.

Test procedure and measurements. After temperature stabilization, bending load was applied at quasi-static loading rate (displacement rate of the ram : 3 mm/min). During the test several measurements were made : applied load, ram displacement, elbow diameter variations (for ovalization), COD in 3 points along the crack length (center, 1/4 and 3/4) and circumferential strains. Direct current electric potential drop method was used to detect crack initiation.

Material characterization

The material property data for the elbow and the connecting pipes were developed using specimens obtained from plates used to make the elbow and the connecting pipes. The material characterization tests consisted of chemical analyses, tensile tests and J-resistance tests. For the pieces which remain elastic during the test, only the Young's modulus is necessary (6 m long pipe : E = 204000 MPa, flange : E = 183 000 MPa).

The chemical composition of the plates is given in Table 1.

TABLE 1 - Chemical composition of the steels (weight %)

	C	Si	Mn	S	P	Ni	Cr	Cu	Al	N2
A48	0.165	0.304	1.150	0.007	0.015	0.069	0.195	0.066	0.037	0.005
A42	0.160	0.221	0.853	0.001	0.008	0.063	0.042	0.024	0.027	0.006

Tensile specimens were machined from plate (A48 steel) and shell (A42 steel). Conventional tensile properties are given in Table 2 and true stress - true strain curves are shown in figure 3.

TABLE 2 - Mechanical properties of the steels at 320°C

	0.2% Offset Yield Strength MPa	Ultimate Tensile Strength MPa	Elongation in 50 mm %	Area Reduction %
A48 (Plate)	194	482	30.7	72.0
A42 (Shell)	153	414	31.5	76.2

J-resistance tests on CT specimens have given the value of $J_{0.2}$ (value of J for 0.2 mm of crack extension). For A48 steel, $J_{0.2}$ is ranging between 240 and 350 kJ/m^2 (depending of the specimen orientation), while for the A42 steel, its value is about 450 to 500 kJ/m^2. For this last steel, the high measured value is due to the very low sulphur and phosphorus content.

EXPERIMENTAL RESULTS

At the end of the test, after 800 mm of ram displacement, the bending moment reached 2800 kN.m and the elbow showed a large ovalization (about 40 mm of diameter variations). Applied load versus ram displacement and COD versus ram displacement curves are shown in figures 4 and 5. No evidence of crack initiation was detected by the d-c e.p. measurements. That was confirmed by the destructive examination : the notch area was cut out from the elbow, then cooled in liquid nitrogen to ensure brittle fracture and finally broken open.

ANALYSES

The numerical analyses are performed using finite element calculations made with the EDF internal code ASTER, in order to calculate the stress intensity factor K and the J-integral. First, an elastic computation of the uncracked structure is made to determine elastic stress field in the elbow. For 100 mm of imposed displacement,

a bending stress σ_b = 414 MPa and a compressive membrane stress σ_m = - 39 MPa are induced in the elbow wall. Then an elastic computation of the cracked structure is made to calculate J_e (and K). The structure is modelled with 15 and 20-node elements and contains about 10000 nodes (figure 6). The 3-D energy release rate G is calculated using the G-THETA method developed by EDF [2]. The evolution of K along the crack front is shown in figure 7 and compared with the values obtained with the influence function method [3,4].

A simplified method [5] derived from the R6 rule is used to calculate the elastic-plastic J knowing the stress intensity factor and the elastic stress distribution in the elbow wall. The comparisons of these J values with those given by CT specimens conclude to the onset of crack initiation before the end of the test. However J FE results obtained on another elbow have shown that this simplified method could overestimate J up to 3 times for large applied displacement.

CONCLUSIONS

A bending test was performed on a large diameter carbon steel elbow containing a semi-elliptical notch on one flank ; despite the large displacement applied, no initiation of the crack occured. The simplified J-estimation scheme used to calculate J concluded to the initiation, but the large conservatism of this method may explain the discrepancy with the experimental result. A non linear finite element calculation of J will be made for definite conclusion.

REFERENCES

[1] Eripret, Ch., Le Delliou, P. and Masson, J.C., "Study of cast duplex stainless steel elbow under closure bending", Proceedings of ECF8, 1990, Vol. 3, pp. 1570-1575.

[2] Wadier, Y. and Malak, O., "The Theta method applied to the analysis of 3D elastic-plastic cracked bodies", Proc. SMIRT 10, Vol. G, pp 13-18, Anaheim, August 1989.

[3] Heliot, J., "Elongated (a/c = 10) longitudinal semi-elliptical crack on the inside surface of a cylinder with t/R_i = 10", Creusot-Loire internal report (in French), Sept. 1979.

[4] Heliot, J., Labbens, R.C. and Pellissier-Tanon, A., "Semi-elliptical cracks in a cylinder subjected to stress gradients" in Fracture Mechanics, ASTM STP 677, 1979, pp. 341-364.

[5] Pellissier-Tanon, A. et al., "Stress classification in industrial fracture mechanics analysis", Proc. 7th ICPVP, Düsseldorf, 1992.

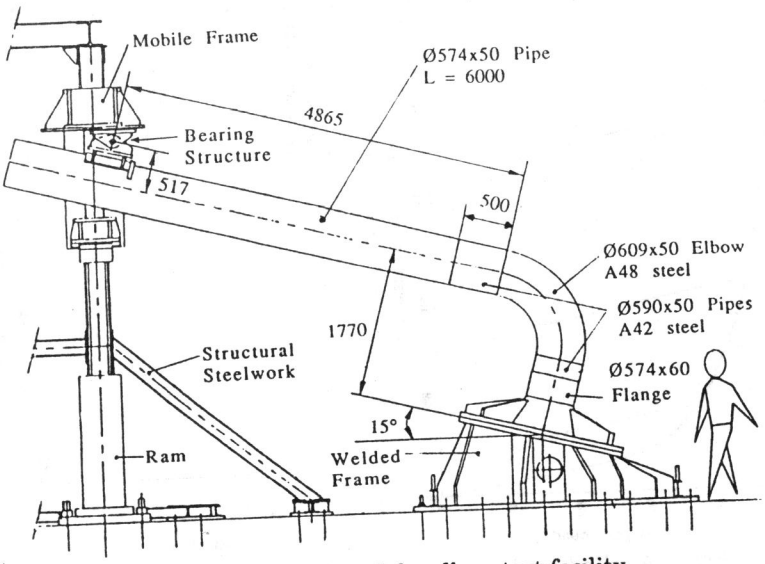

Fig. 1 Schematic of the elbow test facility

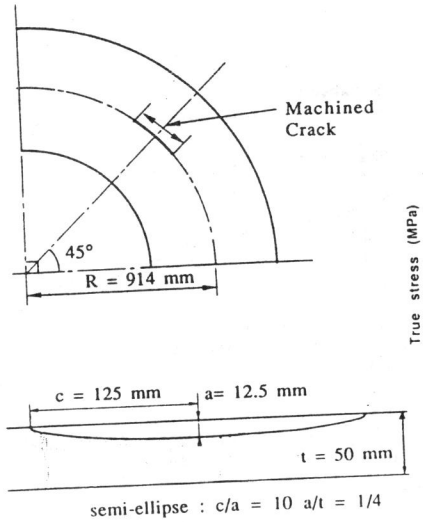

Fig. 2 Schematic of crack geometry

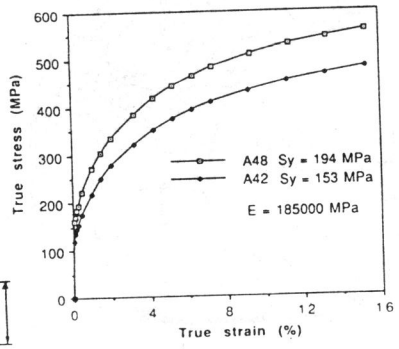

Fig. 3 True stress - true strain curves at 320°C

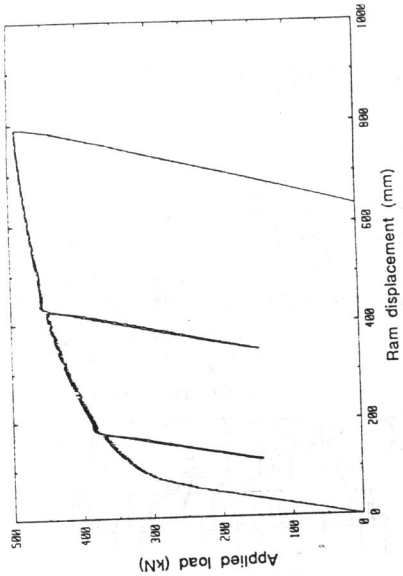

Fig. 4 Applied load versus ram displacement curve

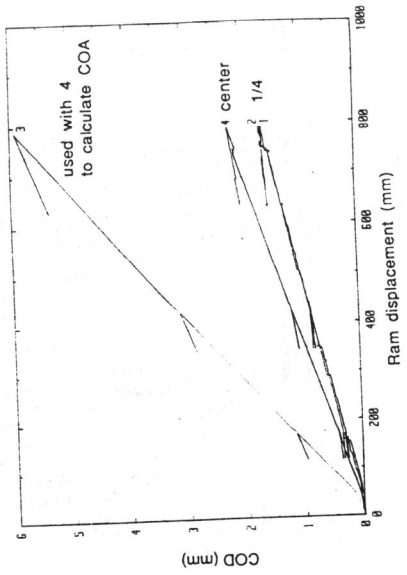

Fig. 5 COD versus ram displacement curves

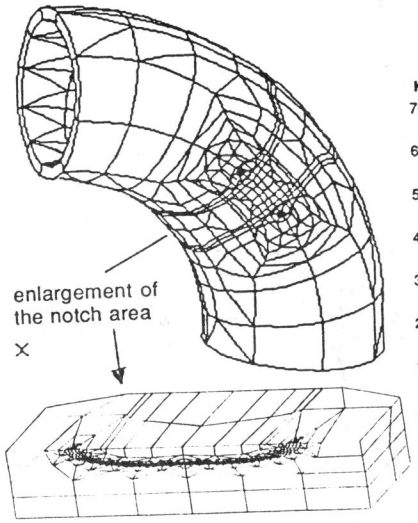

Fig. 6 View of the finite element mesh

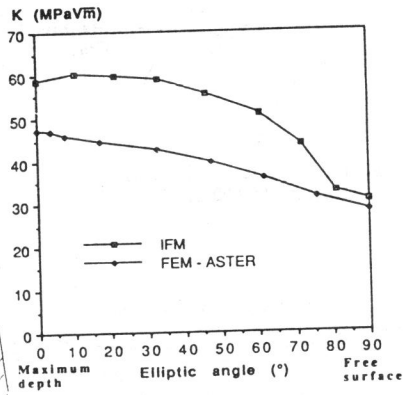

Fig. 7 Evolution of K_I along the crack front for U = 100 mm